Chem

Article

ElectroChemputer with integrated monitoring for programmable electrochemistry

Graphical abstract

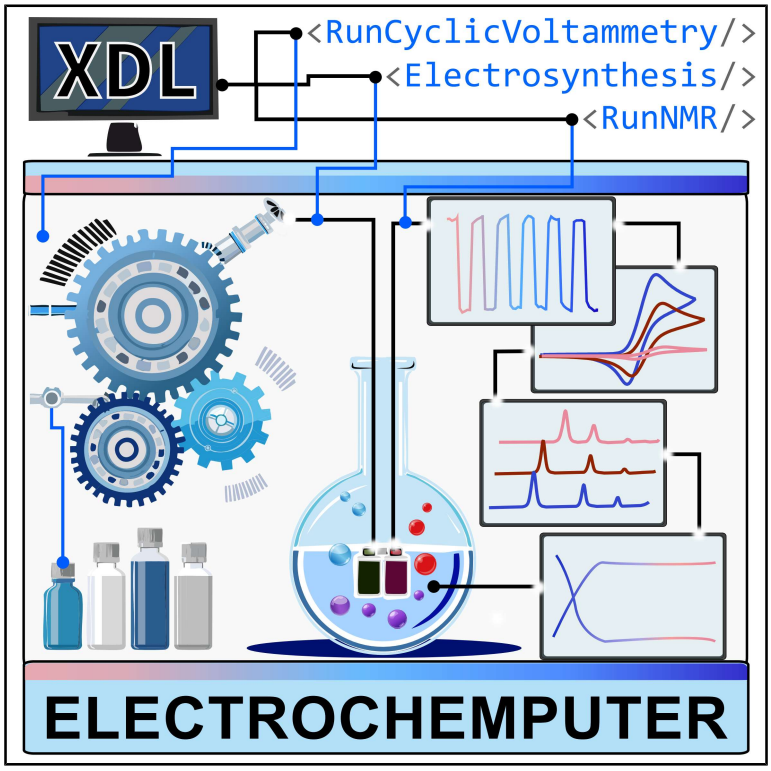

Highlights

- A universal framework for programmable electrosynthesis is established
- The ElectroChemputer integrates real-time monitoring via NMR and electroanalysis
- It allows for parallel multistep reactions through XDL
- It automates complex electrochemical processes for democratized synthesis

Authors

Melanie Guillén Soler, Robert Rauschen, Kristine Laws, Abhishek Sharma, Niclas Grocholski, Mark McNulty, Leroy Cronin

Correspondence

lee.cronin@glasgow.ac.uk

In brief

The ElectroChemputer is a programmable, modular platform that unifies automated electrochemical synthesis with real-time analytical feedback. By integrating nuclear magnetic resonance monitoring with electroanalysis, the system enables the parallel execution of diverse and complex synthetic protocols. This reproducible infrastructure sets a new standard for electrosynthesis.

Guillén Soler et al., 2026, Chem *12*, 102907
March 12, 2026
https://doi.org/10.1016/j.chempr.2025.102907

CellPress

Please cite this article in press as: Guillén Soler et al., ElectroChemputer with integrated monitoring for programmable electrochemistry, Chem (2025), https://doi.org/10.1016/j.chempr.2025.102907

Chem

CellPress
OPEN ACCESS

Article

ElectroChemputer with integrated monitoring for programmable electrochemistry

Melanie Guillén Soler,[1] Robert Rauschen,[1] Kristine Laws,[1] Abhishek Sharma,[1] Niclas Grocholski,[1] Mark McNulty,[1] and Leroy Cronin[1,2,*]

[1]Advanced Research Centre, University of Glasgow, 11 Chapel Lane, Glasgow G11 6EW, UK
[2]Lead contact
*Correspondence: lee.cronin@glasgow.ac.uk
https://doi.org/10.1016/j.chempr.2025.102907

THE BIGGER PICTURE Electro-organic synthesis offers a route to molecules by using electrons in place of stoichiometric reagents, but its promise is still curbed by the sheer diversity of electrochemical cells, electrodes, and control schemes, which complicates reproducibility and scale-up. The ElectroChemputer reframes that challenge as a software problem: it encodes every electrochemical step in our Turing-complete programming XDL language and executes them on a modular hardware backbone while streaming real-time nuclear magnetic resonance (NMR) and electroanalytical data, turning electrosynthesis into a "fly-by-wire" operation. By standardizing hardware, code, and analytics in one open platform, the ElectroChemputer lowers the entry barrier to electrochemistry, enabling researchers to prototype reactions, optimize conditions, and share executable procedures.

SUMMARY

Electrochemical synthesis offers a sustainable and atom-economical alternative to conventional methods. Although recent advances have enabled electrochemical discovery, the integration of real-time control with analysis promises to allow electrochemical "fly by wire." Herein, we present the ElectroChemputer, a programmable, modular standard platform enabling fully automated execution of electrochemical workflows. It integrates nuclear magnetic resonance (NMR) spectroscopy and electroanalytical reaction monitoring to provide structural and quantitative insight into reaction progression. Across 170 h of runtime, the system accumulated >1,500 coordinated unit operations and acquired >600 cyclic voltammograms. The ElectroChemputer enabled real-time stopped-flow NMR monitoring and data analysis of complex processes, such as decarboxylation via alternating polarity. Furthermore, we explored its flexibility for diverse transformations, including nucleophilic substitutions, oxidative couplings, and electrodepositions. By using queues and blueprints, it could run multiple protocols in parallel, demonstrating its adaptability across reaction classes, electrode materials, and configurations. Through its modular architecture, the ElectroChemputer sets the stage for programmable, autonomous, and democratized electrochemical synthesis.

INTRODUCTION

Electrochemical synthesis has recently re-emerged as a powerful strategy for constructing complex organic molecules.[1–3] By using electrons as traceless redox equivalents, electrosynthesis offers a clean and energy-efficient approach to bond formation.[4] Despite its clear potential, broader adoption of organic electrosynthesis remains limited by persistent challenges in experimental standardization and complexity, reproducibility, analytical integration, and the lack of universal, accessible workflows and platforms. A key barrier toward the broader adoption of electrosynthesis lies in the diversity and variability of electrochemical setups, which introduces significant complexity and undermines reproducibility. Unlike thermal or catalytic reactions, where flask geometry or stirring rates are relatively standardized, electrosynthetic outcomes are highly sensitive to a wide array of interdependent physical parameters. Electrode composition, surface area, interelectrode distance, current density, and cell geometry can profoundly influence reaction efficiency, selectivity, and scalability.[5,6] Therefore, in the absence of a standardized language or modular architecture to define and control these variables—or a universal framework to describe and share procedures—reproducibility across laboratories is compromised.

In response to these challenges, recent developments in automated electrochemical platforms have demonstrated the potential for closed-loop experimentation, machine learning, and

Please cite this article in press as: Guillén Soler et al., ElectroChemputer with integrated monitoring for programmable electrochemistry, Chem (2025), https://doi.org/10.1016/j.chempr.2025.102907

modular reactor design to explore reactivity with minimal human input.[7–15] Automation provides a path not only to scale and speed but also to standardization: by explicitly encoding experimental logic and controlling key parameters digitally, automated systems can reduce variability and enhance reproducibility. Yet, most current platforms remain constrained by rigid control architectures, platform-specific implementations, and narrow-scope mechanistic focus. They lack the flexibility required for multistep synthesis, integration with broader synthetic workflows, and real-time insight into molecular progression. Furthermore, although influential for laboratory-scale transformations (such as olefination via alternating polarity [AP]), commercial platforms such as ElectraSyn[9] rely on proprietary software and hardware, limiting interoperability and extensibility.[16]

These limitations underscore a deeper need: a universal programming and execution framework for electrochemistry—one that abstracts the experimental procedures from the underlying hardware and ensures protocol portability, reproducibility, and transparency.[17] We previously introduced the Chemputer together with the Chemical Description Language (XDL, where X is the capital Greek letter chi) as a universal chemical synthesis state machine that can digitally capture synthetic procedures.[18–20] These developments enabled programmable synthetic chemistry through modular hardware and executable digital procedures. Yet, a comparable, standardized automated system tailored specifically for electrochemical synthesis has not been established, and this is a missed opportunity because such a system could autonomously combine robotic synthesis and electrochemical synthesis in one platform. This integrated platform, alongside advances in automation, digital control, and real-time analytical tools, is equally critical to unlocking the full potential of electrosynthesis. Beyond traditional voltammetry or *ex situ* analysis, advanced, on-line analytical tools are essential for gaining deeper insight into electrochemical reaction pathways.[21–27] Previously, real-time, on-line nuclear magnetic resonance (NMR) spectroscopy was particularly insightful for extracting meaningful reaction knowledge without interrupting the electrochemical process.[28,29] However, its application to automated screening remains limited. Cao et al. developed a two-chamber thin-layer liquid-NMR spectroelectrochemical cell that enabled the acquisition of NMR spectra alongside cyclic voltammetry (CV) scans, showcasing how voltage-resolved NMR can track mechanistic changes *in situ*. More recently, NMR was incorporated into fully autonomous Chemputer workflows, which demonstrated that the integration of benchtop NMR spectroscopy into a self-optimizing platform enables multicomponent synthesis with closed-loop feedback.[30] In parallel, refined data-acquisition and post-processing protocols for *in situ* 1D NMR showed that optimized single-scan parameters and dynamic processing strategies can dramatically improve both temporal resolution and signal-to-noise ratios, thus extending the usefulness of NMR for real-time chemical analysis.[31] Although these advances in NMR acquisition and processing have greatly improved the temporal and structural resolution of real-time monitoring, automated interpretation of evolving spectral data remains a bottleneck, particularly in the context of programmable reaction control. To address this, we employ the Jaccard similarity index, a measure of set similarity based on intersection over union (IoU). This index can be adapted for NMR data analysis to quantify spectral or structural similarities. This approach transforms spectral change into a real-time metric, which is well suited for integration into digital workflows.

Through a series of representative electrosynthetic transformations and methodologies—including nucleophilic substitutions, oxidative couplings, multistep synthesis, and electrochemical depositions—we introduce the ElectroChemputer. As seen in Figure 1, this serves as both an electrosynthetic and an analytical automated platform.

Using the new programmable electrochemical XDL steps, we can remotely program and conduct multiparallel electrosynthesis, as well as monitor reactions through CV, accumulated charge, and NMR. In addition, we demonstrate that the system can adapt to a wide array of substrates, configurations, and electrochemical protocols, such as direct current (DC) and AP. At the same time, we report a strategy for analyzing electrochemical reactions *in situ* with NMR. By applying a plateau-detection algorithm to the course of the Jaccard similarity index, we establish an automated endpoint detection, ensuring efficient encoding of reaction times. To the best of our knowledge, this method has not been used in conjunction with electrochemical synthesis before.

RESULTS AND DISCUSSION

The system backbone consists of pumps and valves connected in series via polytetrafluoroethylene (PTFE) tubing.[32] To allow for parallel multistep reactions, we daisy chained the backbone's valves, expanding the number of available ports to accommodate pumps, reagents, waste, reactors, and modules, such as the separator, rotary evaporator, and benchtop NMR.[33] Leveraging the modularity of the system, we extended its capabilities by integrating a programmable power supply, a potentiostat, and a polarity controller for constructing the electrochemical module. These components were interfaced with the ElectroChemputer software interface through XDL, enabling seamless execution of electrochemical workflows together with non-electrochemical operations. The programmable power supply (DP832A, RIGOL Technologies) was selected for its three independent output channels and full programmability, allowing the delivery of constant current or voltage. In addition, the polarity controller allowed the power supply's output voltage polarities to be inverted programmatically as needed (Figures S1 and S2). The potentiostat (SP 150 from Biologic) enabled electrochemical analysis protocols to be encoded and executed via XDL. This integration introduced three key functionalities: autonomous and parallel execution of electrochemical synthetic operations; flexible and scalable control via commercially available multichannel power supplies; and in-line electrochemical characterization with the potential for additional spectroscopic monitoring techniques, such as NMR (Figure 2).

Then, we connected the power supply to independently addressable reaction cells, including custom-built 10 mL V-shaped bottom flasks used as undivided reaction cells and fitted with 3D-printed lids supporting both two- and three-electrode configurations (Figures S3 and S4). The V-shaped bottom of the vials facilitates liquid collection through the PTFE tubing,

Please cite this article in press as: Guillén Soler et al., ElectroChemputer with integrated monitoring for programmable electrochemistry, Chem (2025), https://doi.org/10.1016/j.chempr.2025.102907

CellPress
OPEN ACCESS

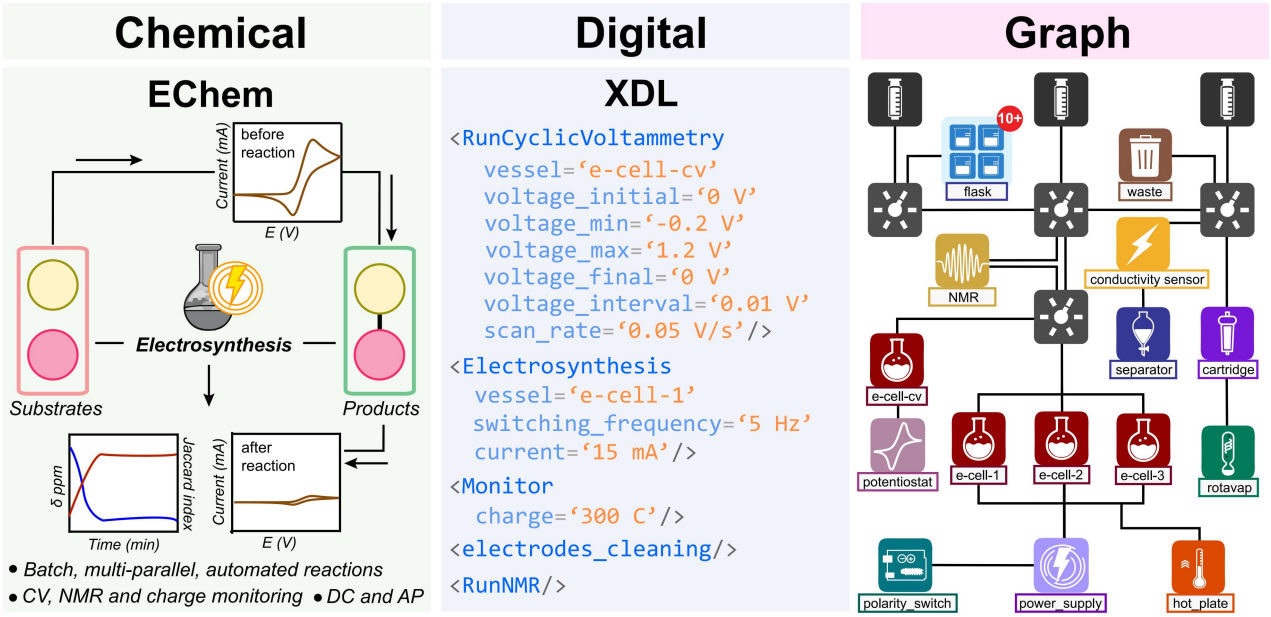

Figure 1. Overview of an integrated approach to organic electrosynthesis combining chemical and digital chemistry through "chemputation"

The platform highlights substrate transformation into products under controlled direct current (DC) or alternating polarity (AP) conditions, monitored via charge, cyclic voltammetry (CV), and NMR. The experimental protocol is translated into XDL. Key parameters, such as voltage, current, and monitoring steps, are defined for automating and standardizing electrosynthesis. The connectivity between hardware modules is encoded in a digital graph that specifies the modules required for the synthetic operations, including a potentiostat, a power supply, a polarity switch, and benchtop NMR.

and the lid supports various electrode materials and geometries (e.g., carbon rods, platinum coiled wires, meshes, and reticulated vitreous carbon foams). Additionally, we used a typical divided H-type electrochemical cell as needed and adapted electrode lids in the same manner as those of the undivided cells (Figures S5 and S6). For parallel screening, we developed a custom electrochemical cell array capable of hosting eight commercial vials (up to 6 mL volume each) with short electrode gaps (3.3 mm) to ensure compact, high-throughput electrochemical testing (Figures S7 and S8). All reaction vessels were sealed and fitted with tubing adapters so we could connect them to the Chemputer backbone. We routed the electrical connections to the potentiostat and the multichannel power supply beneath the fume hood to ensure safe, compact, and organized operation (Figure 2).

To enable programmable electrosynthesis, we developed new XDL steps for controlling both the potentiostat and the power supply. These steps were validated across a series of electrochemical reactions with diverse mechanisms. The general workflow, which will be explained in more detail in the upcoming sections, proceeds as follows: (1) transfer of the reagents to the three-electrode configuration cell, nitrogen purging, and initial CV characterization; (2) transfer of the reaction mixture to the two-electrode configuration cell for electrosynthesis; (3) charge monitoring; and (4) transfer for final CV characterization. Finally, crude reaction mixtures are automatically transferred into the system's purification modules for separation, filtration, and solvent evaporation, enabling fully automated synthesis.

The first case study illustrating the platform's capabilities is the synthesis of 3-formylindoles via the electrochemical decarboxylation of glyoxylic acid (GA) in the presence of an amine catalyst, as previously described in the literature.[34] The experimental procedure can be readily adapted and converted into XDL syntax. This represents the abstraction layer, where high-level chemical operations—such as reagent addition, stirring, electrolysis, or cleaning—are encoded in a standardized, machine-readable format. Once abstracted, the XDL script is processed by the interpreter, which translates each instruction in the context of the available modules in Figure 2. This layer handles the translation from generalized steps to hardware-specific commands, allowing the same script to be executed on different setups. The instructions are then carried out by the hardware layer of the ElectroChemputer system, which includes pumps, valves, sensors, and the electrochemical module (Figure 3). The entire process is controlled by a Python script. An algorithm calculates the optimal current or voltage in advance on the basis of the input reactant quantity and electrode surface area and determines the required total charge to be monitored during the electrochemical reaction. Once these parameters are established, the appropriate XDL script can be manually generated accordingly.

The first step in the workflow involves systematically investigating the redox properties of each reactant and their resulting mixture (Figure 3). The sequence of XDL steps—add, purge, and "RunCyclicVoltammetry"—is executed after the addition of each reactant. This versatile approach facilitates a more efficient examination of the redox features of the system. As shown in Figure S11, the initial exploration of the redox potential window

Please cite this article in press as: Guillén Soler et al., ElectroChemputer with integrated monitoring for programmable electrochemistry, Chem (2025), https://doi.org/10.1016/j.chempr.2025.102907

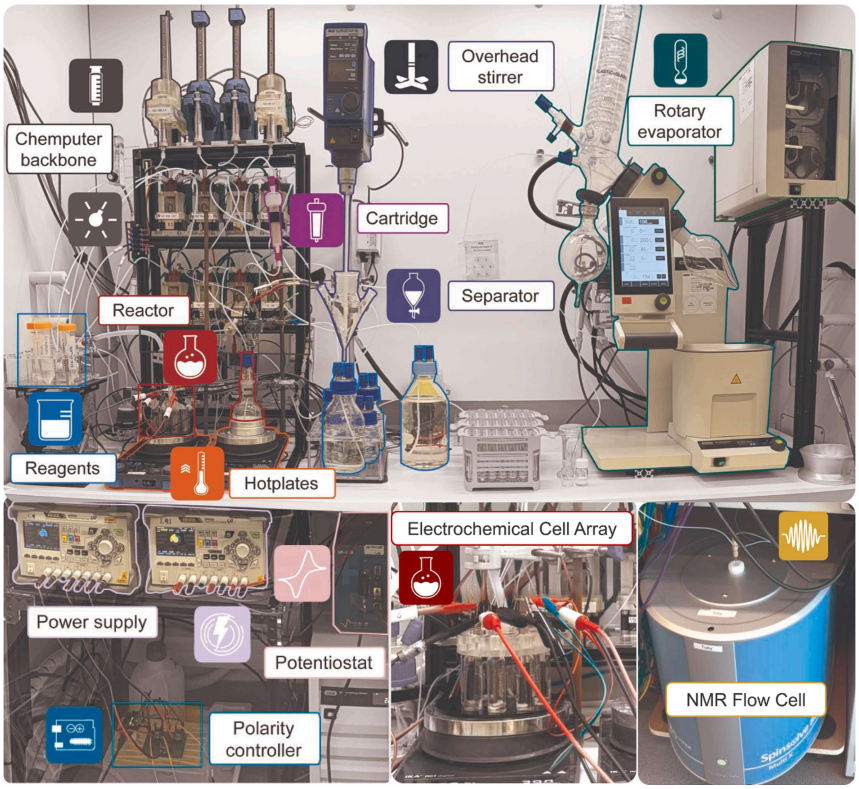

Figure 2. Physical representation of the ElectroChemputer

The modular platform comprises both readily available commercial devices and custom-built items. Icons next to each device correspond to their representations in the XDL graph-based schematic.

can be carried out with the new custom XDL step for CV. Furthermore, consecutive repetitions of specific CV steps with varied parameters can be adjusted in the XDL script. After the initial CV characterization, the reaction mixture is transferred to the reaction vessel connected to the power supply (Figures 3 and S12).

The corresponding "electrosynthesis" XDL step specifies the reactor, the current or voltage, and the time. Additionally, a monitoring step tracks the charge flow during the reaction. This step allows the user to define the specific reactor target and the maximum allowable charge (expressed in coulombs) to be accumulated during the reaction. Once the predefined charge limit is reached, the reaction mixture is redirected back to the reactor connected to the potentiostat for a final round of CV characterization. This step provides critical insights into the state of the reaction, enabling a detailed assessment of its progress and outcomes.

Upon confirmation of reaction completion, the reaction mixture is transferred to the separator, which is agitated by an overhead stirrer for liquid-liquid separation. The phase boundary is detected with a conductivity sensor, and the combined organic layers are transferred to the rotary evaporator after filtration through a cartridge of $MgSO_4$ and sand (1:1) and concentrated. The backbone is cleaned through an automated cleaning routine (reset handling), defined by the user to remove different types of contamination present after different procedures, thus concluding the experimental workflow. It is important to highlight that blueprints have been strategically integrated at specific stages within the XDL workflow to standardize repetitive operational procedures. Blueprints encapsulate an ordered, generalizable sequence of unit operations into a concise single step, in which the parameters, hardware requirements, and reagents have to be defined.[35] In our workflow, we used a blueprint for cleaning the reaction vessel and the electrodes to ensure that the setup was free of contamination and ready for the next measurement. The cleaning process involves the sequential use of various solvents to remove chemical residues, followed by an electrochemical cleaning phase. During this phase, ten repetitions of CV steps remove potential contaminants and restore the electrode surfaces to their optimal state. The appearance of typical peaks, such as the cathodic peak for gold working electrodes, can be used for confirming electrode stability. As an example, Figure S13 shows CV measurements during the cleaning blueprints recorded before and after the reaction.

For the reaction depicted in Figure 3, CV measurements were systematically recorded after the sequential addition of reagents, each preceded by a nitrogen purge lasting 180 s to ensure an inert atmosphere. The sequential-addition CV profiling is the platform's primary mechanism for handling complex mixtures with multiple redox transitions. By observing the distinct peak shifts or appearances upon the addition of each component, we can effectively deconvolute the electrochemical features, ensuring that the operational current or potential targets the desired species. Upon the addition of GA and methylindole, a distinct peak appeared with an onset potential of 1.0 V, signaling redox activity. Interestingly, the subsequent addition of aniline resulted in a notable shift of this onset potential to 0.60 V, strongly suggesting that aniline acts as a catalyst in the reaction. These findings are consistent with the existing literature, which identifies the active catalytic species as the GA-aniline intermediate anion, which has a redox potential of ~0.60 V. We simultaneously investigated two distinct substrates of the reaction described in Figure 3 by using different channels of the power supply. Leveraging the queuing functionality of XDL, we executed the reactions in parallel. Once the redox characteristics of the system were clear, we initiated the electrosynthesis step. Following the reported experimental protocol, we applied a current density of 2 or 3.3 mA cm^{-2} until 3 F/mol was achieved. We sought to utilize the third channel to conduct a completely

Please cite this article in press as: Guillén Soler et al., ElectroChemputer with integrated monitoring for programmable electrochemistry, Chem (2025), https://doi.org/10.1016/j.chempr.2025.102907

CellPress
OPEN ACCESS

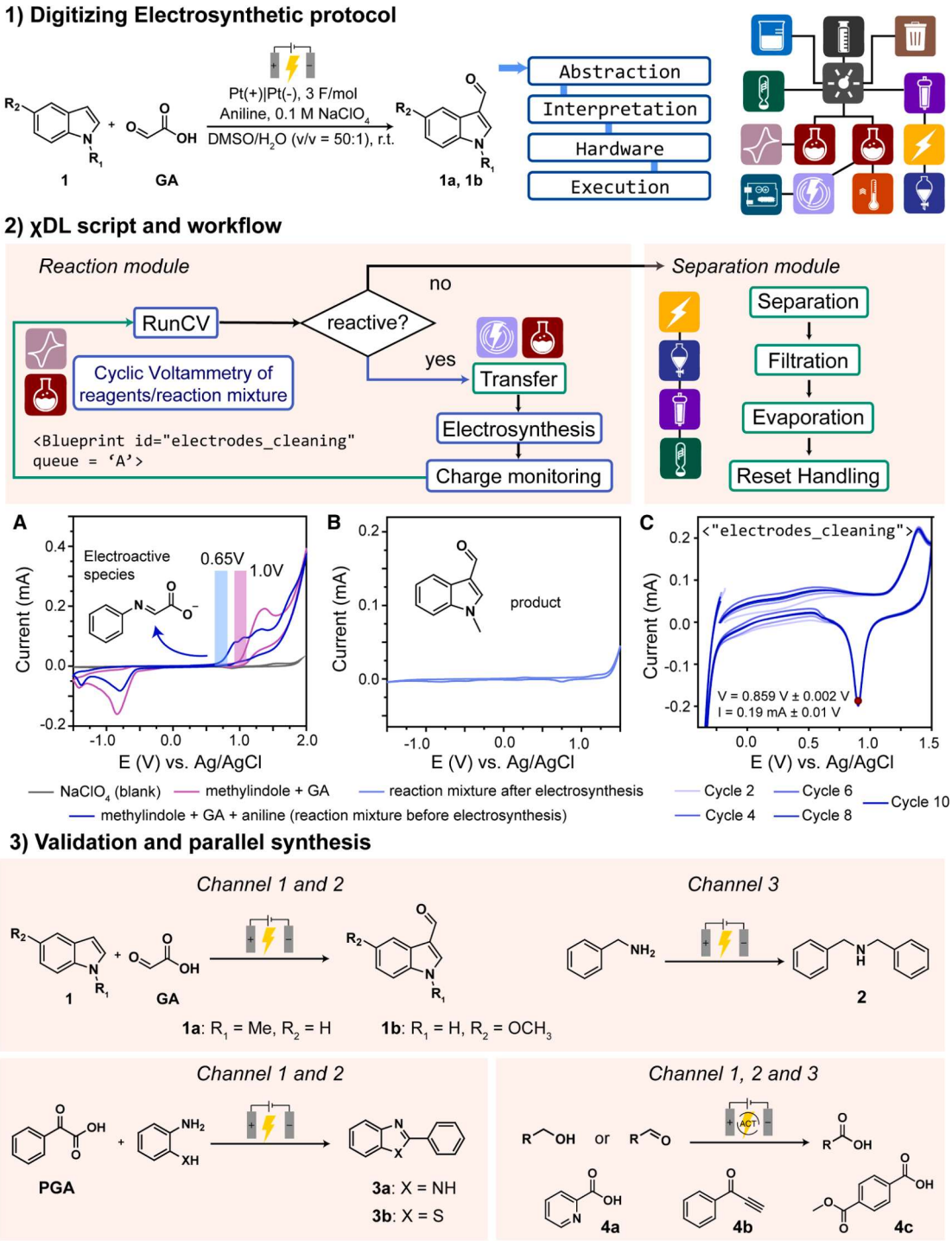

Figure 3. Overview of the proposed framework and workflow in the ElectroChemputer

Starting from a reaction scheme (e.g., the synthesis of 3-formylindoles via electrochemical decarboxylation of glyoxylic acid [GA]), the workflow abstracts a natural language protocol into a machine-readable XDL script. The XDL script is then mapped onto hardware-specific instructions by the platform interpreter and executes the process. The workflow starts with CV profiling of reagents. Then, if the reaction mixture is reactive, it is transferred to the electrosynthesis reactor, where, after reaching the target charge, it comes back to the CV reactor for final CV analysis. If the reaction mixture is no longer reactive, it is transferred to the separation module.

(A and B) CV measurements of the reaction mixture (A) before and (B) after the electrosynthesis.

(C) Electrochemical cleaning of the Au working electrode (WE) via the queued blueprint. The platform was validated through several parallel reactions.

Please cite this article in press as: Guillén Soler et al., ElectroChemputer with integrated monitoring for programmable electrochemistry, Chem (2025), https://doi.org/10.1016/j.chempr.2025.102907

different reaction—an oxidative condensation of benzylamines.[36] The same approach was followed: calculating the electrochemical parameters through the algorithm, adjusting the reaction characteristics to align with our electrode setup, and executing the XDL script. The graph was modified to incorporate the stock solutions and flasks required for the reaction, as well as the third channel of the power supply. Figures S14 and S15 depict the XDL steps and CV measurements of the reactants, and Figure S16 presents the parallel execution of the three reactions. The XDL script for these three parallel reactions runs for 18 h and 46 min, requiring 181 unit operations (including 158 cycles of CV in total). Products **1a**, **1b**, and **2** were obtained after purification in 98%, 96%, and 79% yields, respectively. As such, to demonstrate the reproducibility and versatility of the platform, we aimed to investigate the influence of electrode geometry, surface area, applied current, reaction scale, and interelectrode distance on the yields of reactions **1a**, **1b**, and **2** while maintaining the core logic of the XDL-defined workflow. We dynamically computed the reaction scale, electrode surface area, and current density by using the electrochemical parameterization algorithm and substituted them directly into the digital procedure. The outcomes are summarized in Table S3. Pt mesh electrodes with different surface areas and operated at increased current densities maintained consistently high yields of **1a** (98% and 95%). Combinations of Pt mesh and coiled electrodes at different current densities also delivered **1b** in yields of 96% and 89%, even at different scales. By contrast, a clearer dependence on current and cell volume was seen for product **2**. Higher applied current decreased the yield from 79% to 70%, which suggests reduced selectivity, most likely as a result of overoxidation or uncontrolled side reactivity. Notably, for the same transformation carried out in a cell with reduced volume and interelectrode separation (6 vs. 10 mL, equivalent to 3.3 mm vs. 1.0 cm), the yield improved from 75% to 79%, most likely as a result of enhanced mass transport. This trend agrees with literature reports showing higher yields from microelectrodes than from batch electrochemical cells.[36]

We further validated the ElectroChemputer by carrying out more electrochemical reactions of different natures. The decarboxylative coupling of α-keto acids with *ortho*-amines is a very good example because it demonstrates the platform's ability to facilitate C–heteroatom bond formation under mild, metal-free conditions.[37] This transformation proceeds via anodic oxidation under constant current because the α-keto acid generates a radical intermediate, which subsequently couples with the *ortho*-amine nucleophile. We demonstrated this transformation by using two substrate sets, which afforded benzimidazoles (**3a**) and benzothiazoles (**3b**) in 94% and 90% yields, respectively. Sequential addition of reagents during the CV steps revealed the appearance of oxidation peaks as phenyl GA (PGA) was mixed with the amine; the absence of a corresponding reduction peak suggested irreversible decarboxylation and the formation of acyl radicals via a Kolbe-type mechanism. This is consistent with a mechanistic scenario in which condensation of the acid and amine—possibly facilitated by trifluoroacetic acid (TFA)—precedes decarboxylation. We propose that the electrogenerated *N*,*N*-diisopropylethylamine (DIPEA) serves as a hydrogen atom donor in the final bond-forming step. The recorded CV measurements for **3a** and **3b** (Figures S17 and S18) support the proposed mechanistic pathway and highlight the value of integrating electroanalytical characterization within the system framework. The reactions were carried out in parallel and in separate channels, showcasing the modularity of the system. Over an 18 h period, the ElectroChemputer performed 144 discrete unit operations, including 70 CV scans, emphasizing the robustness and repeatability of the automated workflow. We also investigated the electrode geometry and distance, scale, and current for reactions **3a** and **3b** (Table S4). Overall, the yields were very reproducible even with variation in the parameters. In addition, electrochemical oxidations catalyzed by 4-acetamido-TEMPO (ACT) were successfully validated on the platform.[38] A total of 12 h of the platform and 151 unit operations were used for synthesizing, characterizing, and isolating three different compounds (**4a–4c**). CV analysis of the substrate-catalyst mixtures revealed an anodic peak consistent with the one-electron oxidation of ACT to its oxoammonium form (ACT^+), along with a concomitant attenuation of the cathodic signal, indicative of catalytic turnover. A significant drop in current after the reaction confirmed catalyst consumption and reaction completion (Figure S19), demonstrating the ability of the ElectroChemputer to monitor catalytic efficiency in real time.

Another feature that we added to the platform is the ability to rapidly alternate the polarity of the electrodes. Conventional DC power supplies lack the capability to invert polarities at high frequencies with the precision necessary for rapid AP (rAP) protocols.[16,39–41] To address this limitation, we installed a polarity switch. In XDL terms, we incorporated a parameter for the switching frequency (in hertz) into the electrosynthesis step to define the rate at which the electrode's polarity is reversed (Figure 4).

We explored the electrochemical decarboxylative olefination driven by AP (Figure 4) by protecting the amino group of the starting material in two different ways and subjecting the resulting compound to alternating current. We investigated the platform's ability to integrate and automate a multistep synthetic process where at least one of the synthetic steps is an electrochemical reaction. To coordinate this process, we utilized the queuing system in XDL, which allows multiple synthetic procedures to be defined and executed in parallel. A queue is an ordered set of executable operations assigned to a specific synthetic pathway. Queues ensure that workflows can be run concurrently without conflicts in reagent access, hardware allocation, or process timing.[35]

In this synthesis, the formation of compounds **5c** and **5d** was scheduled in two separate queues ("A" and "B"). Each queue began with a protection step. The steps—from the addition of reagents to the evaporation of each—are sequentially queued. This means that once evaporation in reactor 1 was complete, reactor 2 began its respective separation in parallel with the initiation of the electrosynthesis steps for e-cell-1. These queues can proceed in parallel if there is no contention for shared modules, reagents, or hardware. Building upon Baran's experimental investigations,[41] we executed the reactions depicted in Figure 4, affording products **5a**, **5b**, **5c**, and **5d** in 95%, 88%, 52%, and 87% yields, respectively. The electrochemical characterization exhibited an initial anodic wave, which was attributed to

Please cite this article in press as: Guillén Soler et al., ElectroChemputer with integrated monitoring for programmable electrochemistry, Chem (2025), https://doi.org/10.1016/j.chempr.2025.102907

CellPress
OPEN ACCESS

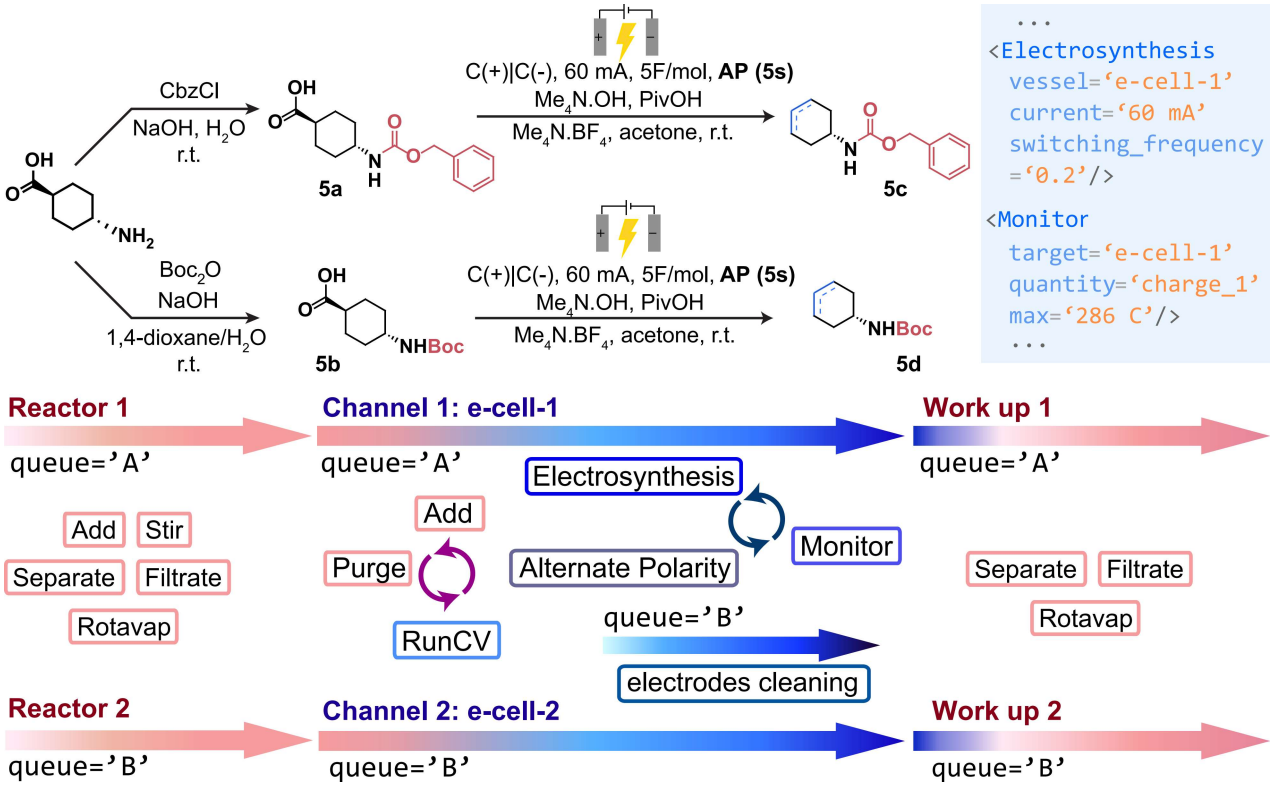

Figure 4. General workflow of batch, multistep synthesis applying AP and queues

Schematic representation of the ElectroChemputer framework applied to electrochemical decarboxylative olefination under AP conditions. The sequential workflow begins with precursor synthesis, followed by programmable electrosynthesis using the polarity controller. XDL-based queuing enables parallel execution of multiple reactions with distinct parameters. Electrosynthesis parameters, polarity-switching frequency, and charge monitoring are integrated into the XDL script.

oxidation of the alkyl carboxylate precursor. After electrosynthesis, that peak was attenuated, indicating substantial conversion (Figure S20).

Control over selectivity in complex electrochemical systems is managed through a multimodal strategy combining digital protocol execution with integrated analytics. The primary method is utilizing sequential CV profiling to systematically deconvolute the mixture. The automated platform and XDL workflow allow for rapid screening of physical parameters (such as current density or electrode surface area) to swiftly locate optimal mass-transport regimes that maximize selectivity, as demonstrated by the yield improvement in the oxidative condensation of benzylamines (reaction 2) (Table S3). Finally, in complex, multicomponent systems, the integrity of the chemical outcome is further verified by integrated, on-line NMR spectroscopy. The Jaccard similarity index quantifies the geometric overlap between spectra by tracking all structural changes in the solution. To enable real-time, high-resolution monitoring of complex electrochemical reactions within an automated setting, we integrated an on-line benchtop NMR spectrometer directly into the ElectroChemputer platform. The overall workflow is illustrated in Figure 5 (top), which schematically depicts the coupling of electrochemical synthesis with on-line NMR acquisition and subsequent data analysis. While applying power to the electrodes, we continuously moved the reaction mixture through the NMR flow cell. At regular intervals (≈1 min), we stopped the flow to acquire single-scan ^{1}H NMR spectra. This allowed us to interrupt the flow only minimally and to preserve temporal resolution for in-depth analysis. We achieved an appropriate signal-to-noise ratio by applying a moving average to the sequence of raw free induction decays (FIDs) before processing them according to established approaches.[31]

This rapid spectroscopic monitoring is complemented by an automated similarity analysis. Specifically, we implemented the Jaccard similarity index as a metric for quantifying the geometric overlap between the spectrum of the initial reaction mixture and the spectra at different time points. Temporal progression of the Jaccard index enables a quantitative assessment of reaction dynamics without prior knowledge of the exact location of diagnostic areas in the spectrum. This makes it particularly useful for an initial characterization of reaction dynamics. Applying a plateau-detection algorithm to this trajectory can help identify stable states in the following way: while the reaction is running, a linear regression is performed on the most recent data points, and if the slope is close to zero, the data are assumed to have reached a plateau region. Nevertheless, the reaction monitoring is continued until the feedback from the electrochemical process signals completion because the plateau in the similarity data

Please cite this article in press as: Guillén Soler et al., ElectroChemputer with integrated monitoring for programmable electrochemistry, Chem (2025), https://doi.org/10.1016/j.chempr.2025.102907

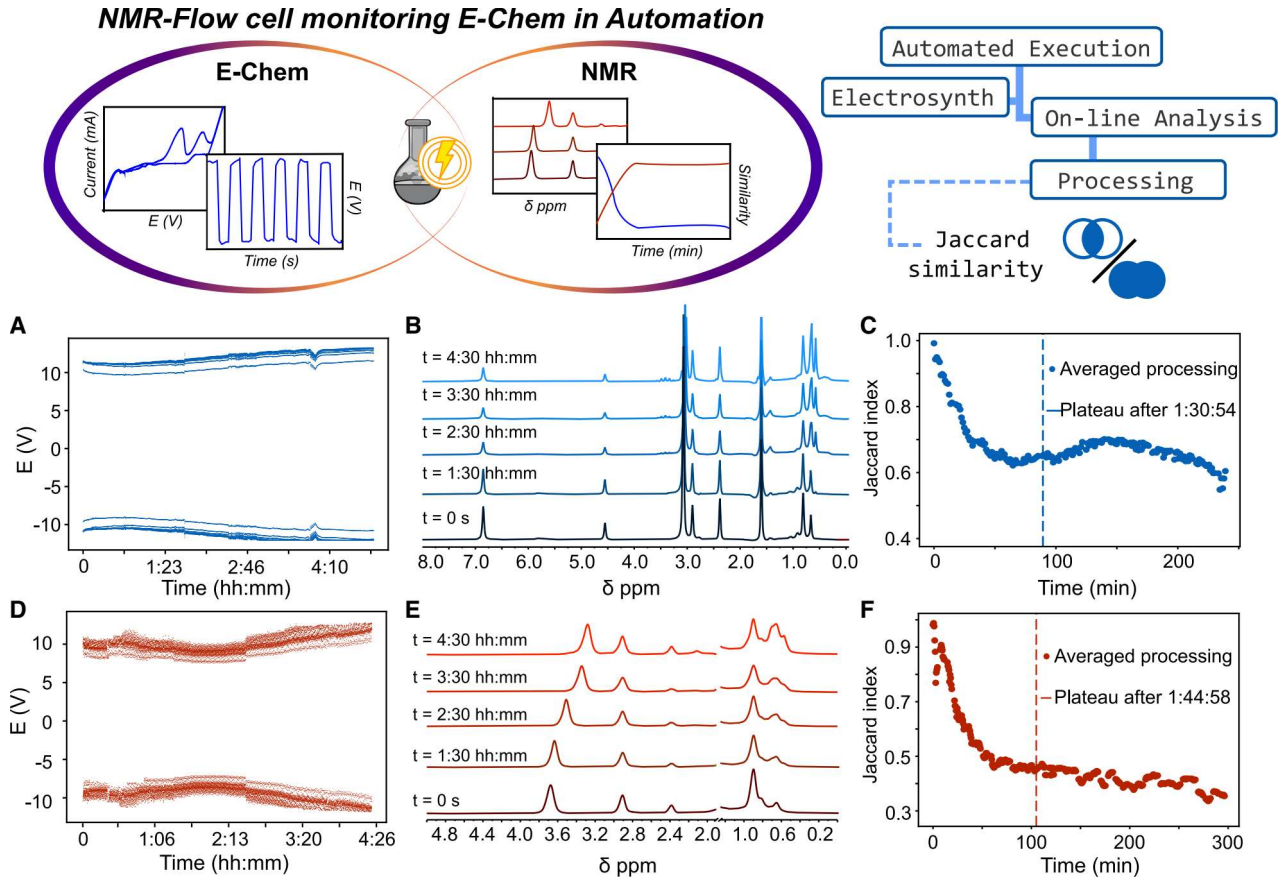

Figure 5. Integration of on-line NMR spectroscopy with electrochemical synthesis monitoring for automated reaction analysis

Top: schematic overview illustrating the coupling of electrochemical processes with on-line NMR analysis within an automated workflow. The next steps include data processing and evaluation through similarity metrics.

(A and D) Chronopotentiometry using AP.

(B and E) NMR spectra of the decarboxylation reactions at different time points.

(C and F) Jaccard similarity index analysis of the NMR spectra over time.

series might only be intermediate (as seen, for example, in Figure 5C).

We evaluated our integrated setup through decarboxylative olefination using rAP. Chronoamperometry with AP (Figures 4A–4D) facilitated stable electrolysis under mild conditions. In the reaction yielding product **5d**, the initial ^{1}H NMR spectrum showed the corresponding peaks of **5b**, electrolyte, pivalic acid, and acetone. As the reaction progressed, the peak at 3.5 ppm shifted upfield (Figure S22A). The evolution of the chemical shift can be analyzed independently of the rest of the spectrum, or it can be followed as part of the Jaccard similarity analysis (Figures 4C–4F and S22). Applying a plateau-detection algorithm to the Jaccard index of the averaged spectra indicated that the reaction reached a stable state after 1 h and 45 min, corresponding to a total charge of 327 C. The isolated, purified product was obtained in 78% yield. Control measurements of the reagents confirmed that the shifting of the peak from 3.5 to 3.1 ppm could be attributed to the changing chemical environment of the hydroxide (in Me_4NOH) as the pH value of the solution increases (Figures S23–S25). Interestingly, the reaction forming **5c** showed different behavior in the NMR monitoring. As the reaction progressed, the hydroxide signal did not appear to shift, but a range of peaks increased or decreased in intensity. The averaged dataset reached a plateau after 1 h and 45 min, corresponding to 378 C, and product **5c** was obtained in 52% yield (Figures S26 and S27). As seen in Figure S28, the chemoselective electrochemical decarboxylation of phthalamide was also monitored via on-line NMR through the same workflow as described previously, and the polarity-switching frequency was adjusted to 100 ms as reported in the literature.[16] Product **6** was obtained in 88% yield after purification, and the corresponding CV characterization is shown in Figure S21.

In addition, we used the ElectroChemputer to produce hydrogen and oxygen gas via electrochemical water splitting, further demonstrating the versatility of the platform. (Splitting water by simply applying a potential difference across two electrodes is environmentally friendly and safe because small quantities of the reactive gases are produced and can be utilized immediately.) We then used the gases as reactants in organic hydrogenation and oxidation reactions. The experimental setup consisted of a two-electrode H-cell configuration connected

Please cite this article in press as: Guillén Soler et al., ElectroChemputer with integrated monitoring for programmable electrochemistry, Chem (2025), https://doi.org/10.1016/j.chempr.2025.102907

CellPress
OPEN ACCESS

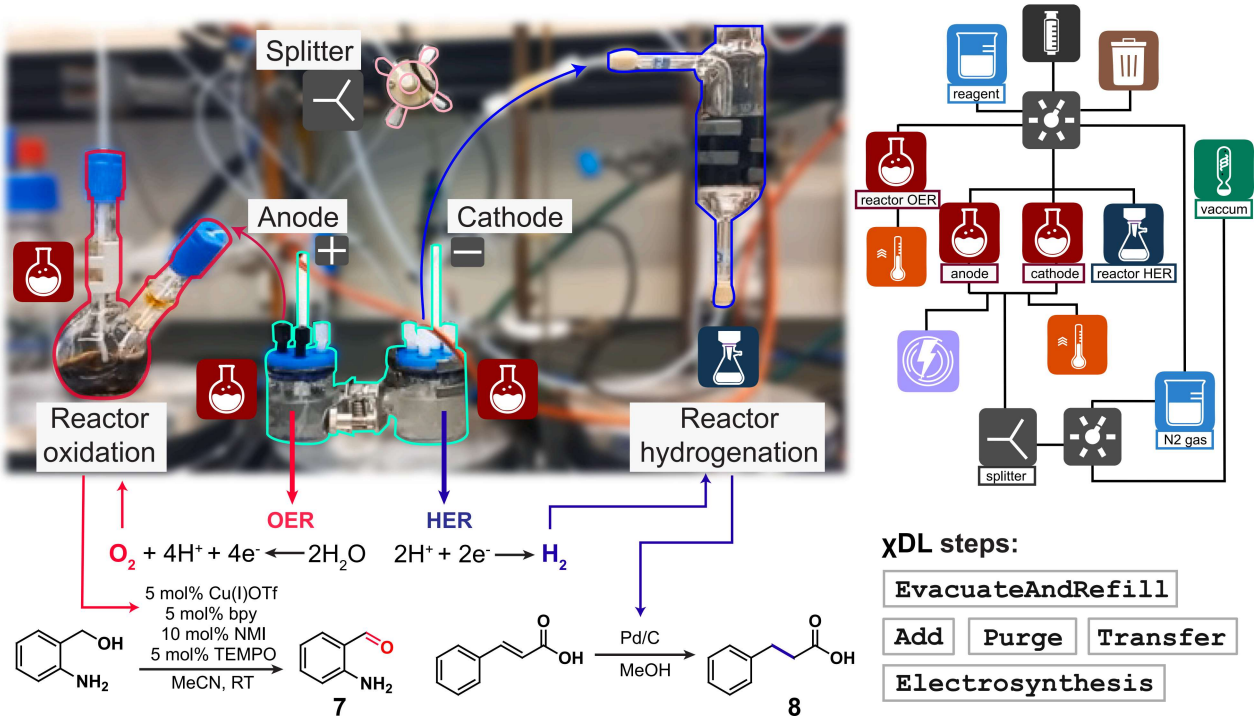

Figure 6. Electrochemical oxidation and hydrogenation with on-site-generated O_2 and H_2 for subsequent organic synthesis

Water electrolysis in a two-chamber H-cell produces H_2 and O_2, which are directly used in automated hydrogenation and oxidation reactions, demonstrating end-to-end integration of electrochemical gas generation with downstream synthetic processes.

via a cation-selective membrane and employing Pt mesh and IrO_2/RuO_2 mesh as the cathode and anode, respectively (Figures 6 and S29). The custom 3D-printed lids for the cell were equipped with four outputs: one for the electrode and three screw fittings for tubing (Figures S5 and S6). The χDL workflow consisted of (1) executing cycles of evacuation and refilling with N_2 gas for all reactors, (2) introducing reactants, and (3) nitrogen purging. The evacuation of air from the cell and replenishment with N_2 gas were crucial steps for preventing oxygen contamination during the reaction. We performed these steps by integrating a nitrogen flask and utilizing the vacuum from a rotary evaporator. Through a single χDL step, "EvacuateAndRefill," we used a valve and a splitter to evacuate both chambers of the H-cell simultaneously and then refill them with N_2. Thereafter, we added the electrolyte to each chamber of the H-cell and further purged the chambers with N_2 gas. We assumed that the oxidation and hydrogenation reactors were properly evacuated and purged simultaneously with the H-cell given that both vessels were sealed and connected to it. Finally, we executed the electrosynthesis step (15 mA for 3 h).

The hydrogen generated from the hydrogen evolution reaction (HER) in the cathodic chamber of the sealed H-cell was channeled through tubing into the hydrogenation reactor (Figure 6). Given the reaction of interest, involving the hydrogenation of a double bond catalyzed by Pd/C, we designed the reactor as a filter-type unit. This filtered reactor simplifies the handling of the Pd/C catalyst because the workup process requires removal of the carbon-based catalyst by filtration. In "reactor oxidation," an alcohol is oxidized to an aldehyde, and this reaction is catalyzed by an *in-situ*-formed Cu species and requires oxygen gas.[42] The necessary oxygen is supplied by the anodic chamber of the H-cell, which performs the oxygen evolution reaction (OER). After electrolysis, both target products (**7** and **8**) were successfully obtained in quantitative yields and characterized.

Yet another feature of the electrochemical platform was demonstrated through electrodepositions of inorganic materials on diverse substrates, including indium tin oxide (ITO) glass and a glassy carbon electrode (GCE). The electrochemical deposition of pyrrole is a well-established technique widely utilized in industry because of the highly conductive nature of the deposited material.[43,44] The deposition process required the use of a three-electrode cell. An initial electrochemical characterization was conducted in a blank experiment with the bare ITO glass substrate in a 0.1 M KNO_3 solution (Figure S30). The characterization comprised the following χDL electrochemical steps: open-circuit voltage (OCV), CV, and electrochemical impedance spectroscopy (EIS) as "RunOpenCircuitVoltage," "RunCyclicVoltammetry," and "RunPEIS," respectively. In the second stage, a pyrrole solution (0.2 M in 0.1 M $NaClO_4$) was transferred to the electrochemical cell, where up to 20 CV cycles were executed. Afterward, a "RunChronoamperometry" step applied 0.8 V for 600 s, and the cell was automatically cleaned as described previously. We then characterized the film by repeating the initial electrochemical steps. We anticipated that the CV would exhibit increased current as a result of the enhanced capacitance and surface area of the deposited film

on the electrode, whereas the EIS would show decreased resistance (Figure S31). The obtained film of polypyrrole (PPy) was successfully deposited on the ITO glass substrate.

Given the success of the method, we further investigated the electrodeposition of metals in the PPy film. We developed a blueprint called "metal electrodeposition" to be executed after the stable and characterized PPy film had been deposited. For application-oriented purposes, this investigation was carried out with a GCE, and the metal of interest was palladium (Pd). The rationale behind this choice was that the electrodeposition of Pd particles from a Pd salt is a well-established process that also enables the exploration of properties such as the electrochemical hydrogen-production capabilities of the film. To achieve the electrodeposition of Pd, we ran the chronoamperometry (CA) and CV steps within the metal-electrodeposition blueprint. We executed multiple iterations of this blueprint in conjunction with the initial characterization stage to assess the film. We identified a typical H-adsorption Pd peak in the 0–0.1 V region, indicating the successful incorporation of Pd within the PPy film (Figure S32).

Conclusions

This study presents the ElectroChemputer as a significant advancement in the automation and digitization of electrochemical synthesis. By extending the Chemputer platform with electrochemical capabilities and embedding electrochemical steps into the XDL syntax, we establish a universal framework for programmable electrosynthesis that is hardware agnostic, reproducible, and highly adaptable. The integration of standardized digital protocols with modular hardware enables seamless control over complex electrochemical workflows, including redox profiling, reaction execution, and analytical characterization.

Through diverse case studies, ranging from nucleophilic substitutions and oxidative couplings to electrocatalytic reactions and electrodepositions, we demonstrate the platform's flexibility across reaction classes, electrode materials, and configurations. The implementation of real-time stopped-flow NMR monitoring and data analysis via the Jaccard similarity index further enhances the platform's ability to quantify reaction progress and automate on-the-fly analysis. Altogether, the system unifies digital chemistry and electrosynthesis, lowering access barriers and enabling broader adoption of electrochemical methods. It establishes a scalable, reproducible infrastructure for innovation in synthetic chemistry, bridging automated experimentation with real-time analytical insight.

METHODS

Detailed methods are provided in the supplemental information.

RESOURCE AVAILABILITY

Lead contact

Further information and requests for resources should be directed to and will be fulfilled by the lead contact, Leroy Cronin (lee.cronin@glasgow.ac.uk).

Materials availability

All materials generated in this study are available from the lead contact without restriction.

Data and code availability

- A dataset of XDL and graph files is provided as Data S2.
- All data reported in this paper will be shared by the lead contact upon request.
- The source code for operating the automated platform is available from the lead contact upon request.
- Any additional information required for reanalyzing the data reported in this paper is available from the lead contact upon request.

ACKNOWLEDGMENTS

We gratefully acknowledge financial support from the Engineering and Physical Sciences Research Council (grants EP/L023652/1, EP/R020914/1, EP/S030603/1, EP/R01308X/1, EP/S017046/1, and EP/S019472/1), the European Research Council (project 670467 SMART-POM), the European Commission (project 766975 MADONNA), and the Defense Advanced Research Projects Agency (projects W911NF-18-2-0036, W911NF-17-1-0316, and HR001119S0003).

AUTHOR CONTRIBUTIONS

L.C. conceived the idea and, together with M.G.S., conceptualized the ElectroChemputer platform. L.C. and M.G.S. managed the project administration and supervised the research. M.G.S. and K.L. developed the methodologies. M.G.S. completed the synthetic work and was primarily responsible for investigation, validation, data curation, and visualization. R.R., N.G., A.S., and M.M., with input from M.G.S., performed software integration and hardware development. R.R. further contributed to the formal analysis and investigation for the NMR experiments, as well as data curation. M.M., N.G., R.R., A.S., and M.G.S. provided the necessary resources underpinning the experimental work. M.G.S. drafted the manuscript, and R.R., A.S., K.L., and L.C. reviewed and edited it. R.R. and K.L. contributed equally to this work.

DECLARATION OF INTERESTS

The authors declare no competing interests.

SUPPLEMENTAL INFORMATION

Supplemental information can be found online at https://doi.org/10.1016/j.chempr.2025.102907.

Received: July 20, 2025
Revised: November 4, 2025
Accepted: December 11, 2025

REFERENCES

1. Zhu, C., Ang, N.W.J., Meyer, T.H., Qiu, Y., and Ackermann, L. (2021). Organic electrochemistry: Molecular syntheses with potential. ACS Cent. Sci. *7*, 415–431. https://doi.org/10.1021/acscentsci.0c01532.
2. Meyer, T.H., Choi, I., Tian, C., and Ackermann, L. (2020). Powering the future: How can electrochemistry make a difference in organic synthesis? Chem *6*, 2484–2496. https://doi.org/10.1016/j.chempr.2020.08.025.
3. Pollok, D., and Waldvogel, S.R. (2020). Electro-organic synthesis – A 21st century technique. Chem. Sci. *11*, 12386–12400. https://doi.org/10.1039/D0SC01848A.
4. Dörr, M., Hielscher, M.M., Proppe, J., and Waldvogel, S.R. (2021). Electrosynthetic screening and modern optimization strategies for electrosynthesis of highly value-added products. ChemElectroChem *8*, 2621–2629. https://doi.org/10.1002/celc.202100318.
5. Perry, S.C., Ponce de León, C., and Walsh, F.C. (2020). Review—The design, performance and continuing development of electrochemical reactors for clean electrosynthesis. J. Electrochem. Soc. *167*, 155525. https://doi.org/10.1149/1945-7111/abc58e.

6. Stephen, H.R., and Röckl, J.L. (2024). The future of electro-organic synthesis in drug discovery and early development. ACS Org. Inorg. Au. *4*, 571–578. https://doi.org/10.1021/acsorginorgau.4c00068.

7. Rial-Rodríguez, E., Williams, J.D., Cantillo, D., Fuchß, T., Sommer, A., Eggenweiler, H.-M., Kappe, C.O., and Laudadio, G. (2024). An automated electrochemical flow platform to accelerate library synthesis and reaction optimization. Angew. Chem. Int. Ed. *63*, e202412045. https://doi.org/10.1002/anie.202412045.

8. Pence, M.A., Hazen, G., and Rodríguez-López, J. (2024). An automated electrochemistry platform for studying pH-dependent molecular electrocatalysis. Digit. Discov. *3*, 1812–1821. https://doi.org/10.1039/D4DD00186A.

9. Schotten, C., Manson, J., Chamberlain, T.W., Bourne, R.A., Nguyen, B.N., Kapur, N., and Willans, C.E. (2022). Development of a multistep, electrochemical flow platform for automated catalyst screening. Catal. Sci. Technol. *12*, 4266–4272. https://doi.org/10.1039/D2CY00587E.

10. Sheng, H., Sun, J., Rodríguez, O., Hoar, B.B., Zhang, W., Xiang, D., Tang, T., Hazra, A., Min, D.S., Doyle, A.G., et al. (2024). Autonomous closed-loop mechanistic investigation of molecular electrochemistry via automation. Nat. Commun. *15*, 2781. https://doi.org/10.1038/s41467-024-47210-x.

11. Pablo-García, S., García, Á., Akkoc, G.D., Sim, M., Cao, Y., Somers, M., Hattrick, C., Yoshikawa, N., Dworschak, D., Hao, H., et al. (2025). An affordable platform for automated synthesis and electrochemical characterization. Device *3*, 100567. https://doi.org/10.1016/j.device.2024.100567.

12. Laws, K., Tze-Kiat Ng, M., Sharma, A., Jiang, Y., Hammer, A.J.S., and Cronin, L. (2024). An autonomous electrochemical discovery robot that utilises probabilistic algorithms: Probing the redox behaviour of inorganic materials. ChemElectroChem *11*, e202300532. https://doi.org/10.1002/celc.202300532.

13. Darvish, K., Skreta, M., Zhao, Y., Yoshikawa, N., Som, S., Bogdanovic, M., Cao, Y., Hao, H., Xu, H., Aspuru-Guzik, A., et al. (2025). ORGANA: A robotic assistant for automated chemistry experimentation and characterization. Matter *8*, 101897. https://doi.org/10.1016/j.matt.2024.10.015.

14. Quinn, H., Robben, G.A., Zheng, Z., Gardner, A.L., Werner, J.G., and Brown, K.A. (2024). PANDA: A self-driving lab for studying electrodeposited polymer films. Mater. Horiz. *11*, 5331–5340. https://doi.org/10.1039/D4MH00797B.

15. Hielscher, M.M., Schneider, J., Lohmann, A.H.J., and Waldvogel, S.R. (2024). Automated optimization of the synthesis of alkyl arenesulfonates in an undivided electrochemical flow cell. ChemElectroChem *11*, e202400360. https://doi.org/10.1002/celc.202400360.

16. Kawamata, Y., Hayashi, K., Carlson, E., Shaji, S., Waldmann, D., Simmons, B.J., Edwards, J.T., Zapf, C.W., Saito, M., and Baran, P.S. (2021). Chemoselective electrosynthesis using rapid alternating polarity. J. Am. Chem. Soc. *143*, 16580–16588. https://doi.org/10.1021/jacs.1c06572.

17. Pence, M.A., Hazen, G., and Rodríguez-López, J. (2025). The emergence of automation in electrochemistry. Curr. Opin. Electrochem. *51*, 101679. https://doi.org/10.1016/j.coelec.2025.101679.

18. Angelone, D., Hammer, A.J.S., Rohrbach, S., Krambeck, S., Granda, J.M., Wolf, J., Zalesskiy, S., Chisholm, G., and Cronin, L. (2021). Convergence of multiple synthetic paradigms in a universally programmable chemical synthesis machine. Nat. Chem. *13*, 63–69. https://doi.org/10.1038/s41557-020-00596-9.

19. Gromski, P.S., Granda, J.M., and Cronin, L. (2020). Universal chemical synthesis and discovery with 'the Chemputer.'. Trends Chem. *2*, 4–12. https://doi.org/10.1016/j.trechm.2019.07.004.

20. Wilbraham, L., Mehr, S.H.M., and Cronin, L. (2021). Digitizing chemistry using the chemical processing unit: From synthesis to discovery. Acc. Chem. Res. *54*, 253–262. https://doi.org/10.1021/acs.accounts.0c00674.

21. Chae, Y., Min, S., Park, E., Lim, C., Cheon, C.-H., Jeong, K., Kwak, K., and Cho, M. (2021). Real-time reaction monitoring with in operando flow NMR and FTIR spectroscopy: Reaction mechanism of benzoxazole synthesis. Anal. Chem. *93*, 2106–2113. https://doi.org/10.1021/acs.analchem.0c03852.

22. Maschmeyer, T., Yunker, L.P.E., and Hein, J.E. (2022). Quantitative and convenient real-time reaction monitoring using stopped-flow benchtop NMR. React. Chem. Eng. *7*, 1061–1072. https://doi.org/10.1039/D2RE00048B.

23. Liu, M., Ni, Z.-R., Sun, H.-J., Cao, S.-H., and Chen, Z. (2021). In situ real-time quantitative determination in electrochemical nuclear magnetic resonance spectroscopy. Sensors *22*, 282. https://doi.org/10.3390/s22010282.

24. Qiu, K., Fato, T.P., Wang, P.-Y., and Long, Y.-T. (2019). Real-time monitoring of electrochemical reactions on single nanoparticles by dark-field and Raman microscopy. Dalton Trans. *48*, 3809–3814. https://doi.org/10.1039/C8DT05141K.

25. Schroeder, C.M., León Sandoval, A., Ohlhorst, K.K., and Leadbeater, N.E. (2023). Development and use of a real-time in-situ monitoring tool for electrochemical advanced oxidation processes. Chem. Methods *3*, e202300014. https://doi.org/10.1002/cmtd.202300014.

26. Khanipour, P., Löffler, M., Reichert, A.M., Haase, F.T., Mayrhofer, K.J.J., and Katsounaros, I. (2019). Electrochemical real-time mass spectrometry (EC-RTMS): Monitoring electrochemical reaction products in real time. Angew. Chem. Int. Ed. *58*, 7273–7277. https://doi.org/10.1002/anie.201901923.

27. Xu, P., and Suntivich, J. (2023). Time-resolved monitoring of electrochemical reactions using in situ stimulated raman spectroscopy. ACS Sustain. Chem. Eng. *11*, 13–17. https://doi.org/10.1021/acssuschemeng.2c04873.

28. Boisseau, R., Bussy, U., Giraudeau, P., and Boujtita, M. (2015). In situ ultrafast 2D NMR spectroelectrochemistry for real-time monitoring of redox reactions. Anal. Chem. *87*, 372–375. https://doi.org/10.1021/ac5041956.

29. Cao, S.-H., Ni, Z.-R., Huang, L., Sun, H.-J., Tang, B., Lin, L.-J., Huang, Y.-Q., Zhou, Z.-Y., Sun, S.-G., and Chen, Z. (2017). In situ monitoring potential-dependent electrochemical process by liquid nmr spectroelectrochemical determination: A proof-of-concept study. Anal. Chem. *89*, 3810–3813. https://doi.org/10.1021/acs.analchem.7b00249.

30. Leonov, A.I., Hammer, A.J.S., Lach, S., Mehr, S.H.M., Caramelli, D., Angelone, D., Khan, A., O'Sullivan, S., Craven, M., Wilbraham, L., et al. (2024). An integrated self-optimizing programmable chemical synthesis and reaction engine. Nat. Commun. *15*, 1240. https://doi.org/10.1038/s41467-024-45444-3.

31. Flook, A., and Lloyd-Jones, G.C. (2024). Simple parameters and data processing for better signal-to-noise and temporal resolution in in situ 1D NMR reaction monitoring. J. Org. Chem. *89*, 16586–16593. https://doi.org/10.1021/acs.joc.4c01882.

32. Rohrbach, S., Šiaučiulis, M., Chisholm, G., Pirvan, P.-A., Saleeb, M., Mehr, S.H.M., Trushina, E., Leonov, A.I., Keenan, G., Khan, A., et al. (2022). Digitization and validation of a chemical synthesis literature database in the ChemPU. Science *377*, 172–180. https://doi.org/10.1126/science.abo0058.

33. Rauschen, R., Ayme, J.-F., Matysiak, B.M., Thomas, D., and Cronin, L. (2025). A programmable modular robot for the synthesis of molecular machines. Chem *11*, 102504. https://doi.org/10.1016/j.chempr.2025.102504.

34. Lin, D.-Z., and Huang, J.-M. (2019). Synthesis of 3-formylindoles via electrochemical decarboxylation of glyoxylic acid with an amine as a dual function organocatalyst. Org. Lett. *21*, 5862–5866. https://doi.org/10.1021/acs.orglett.9b01971.

35. Šiaučiulis, M., Knittl-Frank, C., M Mehr, S.H., Clarke, E., and Cronin, L. (2024). Reaction blueprints and logical control flow for parallelized chiral synthesis in the Chemputer. Nat. Commun. *15*, 10261. https://doi.org/10.1038/s41467-024-54238-6.

36. Amemiya, F., Kashiwagi, T., Fuchigami, T., and Atobe, M. (2011). Electrochemical conversion of benzylamine to dibenzylamine using a microreactor: Analogous system of photocatalytic redox combined synthesis. Chem. Lett. *40*, 606–608. https://doi.org/10.1246/cl.2011.606.

37. Wang, H.-B., and Huang, J.-M. (2016). Decarboxylative coupling of α-keto acids with *ortho*-phenylenediamines promoted by an electrochemical method in aqueous media. Adv. Synth. Catal. *358*, 1975–1981. https://doi.org/10.1002/adsc.201501167.

38. Rafiee, M., Konz, Z.M., Graaf, M.D., Koolman, H.F., and Stahl, S.S. (2018). Electrochemical oxidation of alcohols and aldehydes to carboxylic acids catalyzed by 4-acetamido-TEMPO: An alternative to "Anelli" and "Pinnick" oxidations. ACS Catal. *8*, 6738–6744. https://doi.org/10.1021/acscatal.8b01640.

39. Schotten, C., Taylor, C.J., Bourne, R.A., Chamberlain, T.W., Nguyen, B.N., Kapur, N., and Willans, C.E. (2021). Alternating polarity for enhanced electrochemical synthesis. React. Chem. Eng. *6*, 147–151. https://doi.org/10.1039/D0RE00399A.

40. Fors, S.A., Yap, Y.J., and Malapit, C.A. (2025). Effect of alternating polarity in electrochemical olefin hydrocarboxylation. Angew. Chem. Int. Ed. *64*, e202424865. https://doi.org/10.1002/anie.202424865.

41. Garrido-Castro, A.F., Hioki, Y., Kusumoto, Y., Hayashi, K., Griffin, J., Harper, K.C., Kawamata, Y., and Baran, P.S. (2023). Scalable electrochemical decarboxylative olefination driven by alternating polarity. Angew. Chem. Int. Ed. *62*, e202309157. https://doi.org/10.1002/anie.202309157.

42. Greene, J.F., Hoover, J.M., Mannel, D.S., Root, T.W., and Stahl, S.S. (2013). Continuous-flow aerobic oxidation of primary alcohols with a copper(I)/TEMPO catalyst. Org. Process Res. Dev. *17*, 1247–1251. https://doi.org/10.1021/op400207f.

43. Czichy, M., Zhylitskaya, H., Zassowski, P., Navakouski, M., Chulkin, P., Janasik, P., Lapkowski, M., and Stępień, M. (2020). Electrochemical polymerization of pyrrole–perimidine hybrids: Low-band-gap materials with high n-doping activity. J. Phys. Chem. C *124*, 14350–14362. https://doi.org/10.1021/acs.jpcc.0c03002.

44. Kim, S., Jang, L.K., Park, H.S., and Lee, J.Y. (2016). Electrochemical deposition of conductive and adhesive polypyrrole-dopamine films. Sci. Rep. *6*, 30475. https://doi.org/10.1038/srep30475.